# Cooperative Adaptive Cruise Control in a Mixed-autonomy Traffic System: A Hybrid Stochastic Predictive Approach Incorporating Lane Change

Sahand Mosharafian and Javad Mohammadpour Velni, Senior Member, IEEE

Abstract—This paper presents a stochastic and predictive control design approach for connected and automated vehicles (CAVs) in a mixed-autonomy traffic environment, where CAVs are able to react properly to uncertain maneuvers of humandriven vehicles (HVs). The proposed fully-automated cooperative adaptive cruise control (CACC) design leverages a discrete hybrid stochastic model predictive controller that automatically determines the vehicle's operating mode based on onboard sensors data and information received through vehicle-to-vehicle (V2V) communication. Operating modes include free following, warning, danger, emergency braking, and lane change. Although the controller mainly focuses on maintaining the desired velocity and distance among CAVs, it also allows HVs to perform lane-change maneuvers and merge into the platoon's lane when needed. In response to an HV's position in the lane and its probabilistic behavior, the controller may switch the CAV's operating mode to react accordingly. Considering free-following and emergencybraking modes leads to efficient and safe autonomous driving. Switching between warning, danger, and lane-change modes along with adjusting the steering angle to perform a lane-change maneuver, when needed, robustifies the platoon's performance against unexpected human-driven vehicle maneuvers. Simulation studies are conducted to validate the efficacy of the proposed control design approach. The performance of the proposed control design approach is also compared to a switching control using simulation studies.

Index Terms—Cooperative adaptive cruise control, connected and automated vehicles, model predictive control, discrete hybrid stochastic automata, automated lane change, mixed-autonomy

#### I. INTRODUCTION

Car accidents account for numerous injuries and deaths, most of which are resulted from human errors and can be avoided by leveraging autonomous driving systems [1]. Modern vehicles are equipped with different driver assistance systems that are capable of improving the traffic network by increasing the road capacity and facilitating driving [2]. By increasing the popularity and demand for autonomous vehicles, vehicle platooning in highways and roads would be a possible solution to increase the efficiency and safety of the traffic system. The

Copyright (c) 2022 IEEE. Personal use of this material is permitted. However, permission to use this material for any other purposes must be obtained from the IEEE by sending a request to pubs-permissions@ieee.org.

main goal in the longitudinal vehicle platoon control is to enhance performance while preserving safety.

Lane change is a common driving maneuver performed for different reasons, such as approaching a specific exit or passing a slow-moving vehicle. Inappropriate lane change would result in fatal accidents. The acquisition of onboard sensors data and the information received through vehicle-to-vehicle (V2V) communication would facilitate safety and comfort during a lane-change maneuver [3]. According to [4], an automated lane-change maneuver consists of three stages: decision making (e.g., see [3], [5], [6]), trajectory planning (e.g., see [7], [8]), and control (e.g., see [3], [8]). A Vehicle needs to decide when and how to perform the lane change, and the controller is responsible for tracking the expected trajectory.

Numerous researchers have concentrated on the problem of trajectory planning and control for a safe and efficient lane-change maneuver for autonomous vehicles [1]. The study in [8] presents a collision-free trajectory planning and tracking approach incorporating data collected using sensors and V2V communication. Authors in [9] proposed a lane-change scheduling for a single autonomous vehicle (AV) in a vehicle network consisting of human-driven vehicles (HVs). The goal is for the AV to perform a lane change while not disturbing the moving traffic as far as possible. In [4], a three-layer trajectory planner is presented, in which the first planner (layer) generates a trajectory with some assumptions; when those assumptions are violated, it uses the next trajectory planner (layer) to preserve safety. Authors in [3], proposed a cooperative lane-change method where vehicles communicate with others if a vehicle intends to perform a lane change. The method proposed in [10] allows vehicles to merge to the main road easily as they cooperate with the vehicles already driving on the main road through V2V communication. Authors in [11] presented an approach to adapt AVs' behavior on the main road to facilitate the possible merging of other vehicles.

Communication among vehicles allows cooperative maneuvers and collective awareness. Longitudinal control approaches can be categorized into five groups based on the use of external information: predictive cruise control, adaptive cruise control, urban cruise control, cooperative adaptive cruise control, and connected cruise control [12]. Wireless communication among vehicles enables cooperative adaptive cruise control (CACC), which allows vehicles to safely move close to their preceding

<sup>\*</sup>This work was financially supported by the US National Science Foundation under award CNS-1931981.

S. Mosharafian and J. Mohammadpour Velni are with School of Electrical and Computer Engineering, University of Georgia, GA 30602 United States.

vehicle. Although the primary goal of CACC was to comfort the driving experience, it has proven to improve the traffic system [13]. CACC approaches can be divided into two categories: state feedback control methods (e.g., [14]–[17]), and constrained optimization methods which have more recently evolved to model predictive control (MPC) (e.g., [18]–[20]). State feedback-based methods enable explicit system stability analysis while constrained optimization methods allow considering multiple performance indices subject to hard constraints on the system dynamics and physical limitations of the vehicle [18]. Traditional MPC schemes are formulated in a centralized setting. However, due to the practical limitations for gathering data and the large size of the optimization problem, distributed MPC has emerged to address the limitations of centralized methods [21].

A merging assistant method aiming at improving traffic flow in mixed autonomy is introduced in [22], where the traffic includes HVs and CACC-equipped vehicles in the main lane, while the vehicles on the ramp are HVs. It is assumed that if the CAV's preceding vehicle is an HV, the CAV's controller degrades to adaptive cruise control. For the CACC problem in [23], the platoon leader uses hidden Markov models to detect possible danger in front of it (an adjacent vehicle's cut-in maneuver) and employs that information for its MPC design to act accordingly. Authors in [24] proposed a hybrid MPC scheme including three operating modes for connected and automated vehicles (CAVs) in a platoon to accommodate a number of CAVs in the adjacent lane when performing a lane-change maneuver. A CAV (or a number of CAVs) communicates with the vehicles in the platoon in the target lane so that the platoon makes enough space for a safe and smooth lane change.

In the existing literature, lane-change maneuvers have been investigated from different viewpoints, namely how an AV performs a collision-free lane change and how an AV or a platoon of CAVs react when an adjacent vehicle decides to change its lane to robustify the traffic flow against lane-change maneuvers. However, the problem of robustifying cooperative driving against HVs' maneuvers and maintaining the desired formation and spacing among vehicles in CACC and platooning in the mixed autonomy is not properly addressed. To this aim, this paper extends the controller design approach proposed in [25] by integrating five operating modes, namely free following, warning, danger, emergency braking, and lane change, into a stochastic hybrid MPC scheme for the CACC applications. The controller mainly focuses on maintaining the desired velocity and distance among CAVs while allowing HVs to perform lane change and merge into the platoon's lane when needed. In response to an HV's location and probabilistic behavior, the controller may switch the CAV's operating mode to react accordingly. This fully automated approach results in keeping the behavior of the CAVs in the platoon close to the desired case where the traffic environment is not fully automated.

The following summarizes the contributions of the paper. This work presents a fully automated CACC design in the *mixed autonomy* by leveraging a *discrete hybrid stochastic model predictive controller* that automatically determines the

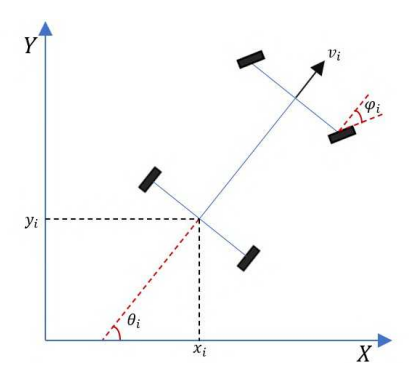


Fig. 1: Vehicle's bicycle model.

vehicle's operating mode based on the onboard sensors data and the information received through V2V communication. Considering free-following and emergency-braking modes leads to efficient and safe autonomous driving. The controller's capability to automatically switch between warning, danger, and lane-change modes, as well as adjust the steering angle to perform a lane-change maneuver when needed, robustifies the platoon performance against unexpected human-driven vehicle maneuvers.

The remainder of the paper is organized as follows. In Section II, the system model and a brief introduction to discrete hybrid stochastic automata are presented. System equations, system constraints, and operating modes are presented in mixed logical dynamical form in Section III. Section IV elaborates on the proposed model predictive control design scheme. Simulation results and evaluation of the proposed controller's performance are provided in Section V. Finally, concluding remarks are made in Section VI.

#### II. PRELIMINARIES

This section describes the dynamic model of vehicles considered in this study and reviews the stochastic and hybrid framework with which the control design problem is formulated.

### A. Description of the System Model

In this work, autonomous vehicles' longitudinal and lateral movements are studied. The goal of each vehicle in longitudinal movement is to reach a relatively small headway while preserving safety during sudden changes in the platoon, e.g., sudden deceleration or sudden lane change performed by adjacent HVs. When an HV enters the CAVs' platoon, CAVs may require a lane change to pass the interrupting HV and achieve their desired distance from their predecessor.

A linear kinematic bicycle model is considered integrating each vehicle longitudinal and lateral movements. According to Fig. 1, the  $i^{th}$  vehicle's bicycle model is represented as

$$\dot{\mathbf{X}}_{i}^{m}(t) = \begin{bmatrix} \dot{x}_{i}(t) \\ \dot{y}_{i}(t) \\ \dot{\theta}_{i}(t) \end{bmatrix} = \begin{bmatrix} \cos(\theta_{i}(t)) \\ \sin(\theta_{i}(t)) \\ u_{i}^{\varphi}(t) \end{bmatrix} v_{i}(t),$$

$$u_{i}^{\varphi}(t) = \frac{\tan(\varphi_{i}(t))}{l_{i}^{w}},$$
(1)

where  $x_i$  and  $y_i$  indicate the vehicle's longitudinal and lateral location from a specified reference, respectively,  $\varphi_i$  is steering angle,  $\theta_i$  is the vehicle's body angle with the X-axis,  $v_i$  is the vehicle's velocity, and the input  $u_i^{\varphi}$  denotes the steering rate. If  $\theta_i$  remains small ( $|\theta_i| << 1$ ), then differential equations in (1) can be rewritten as

$$\dot{\mathbf{X}}_{i}^{m}(t) \approx \begin{bmatrix} 1\\ \theta_{i}(t)\\ u_{i}^{\varphi}(t) \end{bmatrix} v_{i}(t). \tag{2}$$

Two assumptions are made to get rid of the nonlinear differential equations in (2) (these assumptions are later used for solving the MPC problem) which are as follows

$$\dot{\theta}_i(t) \approx u_2(t) \, v_i(t_0), 
\dot{y}_i(t) \approx \theta(t) \, v_i(t_0), 
\forall t_0 < t < t_0 + t_N,$$
(3)

where  $t_0$  defines current time and  $t_N$  is the prediction horizon. Finally, (1) turns into

$$\dot{\mathbf{X}}_{i}^{m}(t) \approx \begin{bmatrix} v_{i}(t) \\ \theta_{i}(t) \, v_{i}(t_{0}) \\ u_{i}^{\varphi}(t) \, v_{i}(t_{0}) \end{bmatrix}. \tag{4}$$

A CACC system with  $N_v$  CAVs is considered in this paper, where  $i \in \{0,1,\dots,N_v-1\}$  represents the  $i^{th}$  vehicle (CAV $_i$ ), and i=0 is the leader vehicle. The distance between  $i^{th}$  vehicle and its preceding vehicle at time t is denoted by  $d_i(t)$  and defined as

$$d_i(t) = x_{i-1}(t) - x_i(t) - l_i^v, (5)$$

where  $x_i$  and  $l_i^v$  are the longitude of the  $i^{th}$  CAV's rear bumper, and the length of the  $i^{th}$  vehicle, respectively. A fixed time headway gap spacing policy, which can improve the string stability and safety [26], is considered as follows

$$d_i^*(t) = T_i v_i(t) + d_i^0, (6)$$

where  $T_i$  is the time gap, and  $d_i^0$  is the standstill distance. The difference between the gap and its desired value is defined as  $\Delta d_i(t) = d_i(t) - d_i^*(t)$ , Hence,  $\Delta \dot{d}_i$  turns into  $\Delta \dot{d}_i(t) = v_{i-1}(t) - v_i(t) - T_i \, a_i(t)$ , where  $a_i$  denotes the acceleration of the  $i^{th}$  vehicle. By taking the driveline dynamics  $\tau_i$  into account, the derivative of the acceleration for vehicle i is  $\dot{a}_i(t) = -\frac{1}{\tau_i} a_i(t) + \frac{1}{\tau_i} u_i^a(t)$ , where  $u_i^a(t)$  acts as the vehicle's acceleration input.

By considering  $x_i(t) = [\Delta d_i(t) \ y_i(t) \ \theta_i(t) \ v_i(t) \ a_i(t)]^T$  as the state vector, the state-space representation for CAV<sub>i</sub>

becomes

For the leader vehicle (i=0), the term  $v_{i-1}(t)$  in (7) is replaced by its desired speed trajectory. Using forward-time approximation for the first-order derivative, (7) can be expressed in discrete time as

$$x_i(k+1) = (I+t_s A_i) x_i(k) + t_s B_i u_i(k) + t_s C_i v_{i-1}(k),$$
 (8)

where I is the identity matrix and  $t_s$  is the sampling time.

#### B. Introduction to Discrete Hybrid Stochastic Automata

Discrete hybrid stochastic automata (DHSA) models a stochastic system including binary and continuous variables. According to [27], a DHSA consists of four components:

1) a switched affine system described by linear difference equations:

$$x_c(k+1) = A_{i(k)}x_c(k) + B_{i(k)}u_c(k) + f_{i(k)}(k),$$
 (9)

where i(k) is the mode of the system,  $x_c(k)$  is the vector of continuous states, and  $u_c(k)$  is the vector of continuous inputs. In the CACC application, the switched affine system represents the vehicle's state-space equations.

2) an event generator which generates a binary output  $\delta_e(k) = f_{EG}(x_c(k), u_c(k))$  such that

$$f_{EG}(x_c, u_c) = 1 \iff H_e x_c + J_e u_c + K_e \le 0, (10)$$

where  $H_e$ ,  $J_e$ , and  $K_e$  are constant matrices representing state weights, input weights, and bias in linear event generator inequalities, respectively. Event generators impact the operating mode of the system. In our CACC formulation, it is assumed that each vehicle has five operating modes, namely free following, warning, emergency braking, danger, and lane change. The event generators for the aforementioned modes are explained in the next section.

3) a mode selector that defines the mode of the system using the following equation

$$i(k) = f_{MS}(x_b(k), u_b(k), \delta_e(k)),$$
 (11)

where  $f_{MS}$  is a Boolean function, and  $x_b(k)$  and  $u_b(k)$  are vector of binary states and binary inputs, respectively.

4

4) a finite state machine (FSM) that represents the stochastic transition from a binary state vector to another one and is described by

$$P[x_b(k+1) = \hat{x}_b] = f_{sFSM}(x_b(k), u_b(k), \delta_e(k), \hat{x}_b),$$

where P denotes the probability. If  $P[x_b(k+1)]$  is nonzero, then the transition is enabled for  $(u_b(k), \delta_e(k))$ . Besides, if more than one transition are enabled for  $(u_b(k), \delta_e(k))$ , they are called conflicting on  $(x_b(k), u_b(k), \delta_e(k))$ . In our CACC problem, the unpredictable behavior of HVs, namely lane change, builds the finite state machine.

In DHSA, the stochastic finite state machine can be replaced using a set of auxiliary binary variables  $w_i(k)$  called uncontrollable events. Hence, a DHSA can be converted to discrete hybrid automata with uncontrollable events. The uncontrollable events for l-1 possible transitions are defined as (for i=1,...,l-1)

$$P[w_i = 1] = p_i = f_{sFSM}(x_b(k), u_b(k), \delta_e(k), \hat{x}_b)$$
 (12)

which means that the  $i^{th}$  transition  $(x_b, u_b, \delta_e) \to \hat{x_b}$  happens if and only if  $w_i = 1$ . Besides,  $w_l = 1$  means that the transition is deterministic. If  $W_s$  represents the indices of the conflicting transitions on  $x_b(k), u_b(k), \delta_e(k)$ , the following equality should hold for  $W_s$ 

$$\sum_{i \in W_s} w_i(k) = 1. \tag{13}$$

If  $\pi(k)$  defines the probability of the transition occurred by w(k), the probability of a trajectory can be calculated using

$$\pi(\mathbf{w}_i) = \prod_{k=0}^{N-1} \pi(k), \tag{14}$$

where  $\mathbf{w}_i$  is the vector of all uncontrollable events. By defining new auxiliary variables, a DHSA can be represented in the mixed logical dynamical (MLD) form [28]. Furthermore, (14) can be rewritten in logarithmic form as

$$\ln(\pi(\mathbf{w}_i)) = \sum_{l=0}^{N-1} \sum_{i=1}^{l} w_i(k) \ln(p_i).$$
 (15)

For eliminating trajectories with small probability, the following chance constraint is added to the system

$$\ln(\pi(\mathbf{w}_i)) \ge \ln(\tilde{p}),\tag{16}$$

where  $0 \le \tilde{p} \le 1$  is the probability bound. Hence, the cost function for a DHSA can be defined as

$$J(\mathbf{u}, \mathbf{w}, \mathbf{r}, x(0)) = J_n - q^p \ln(\pi(\mathbf{w})), \tag{17}$$

where  ${\bf u}$  is the vector of system inputs (within the prediction horizon),  ${\bf r}$  is the vector of desired outputs,  $J_p$  is the performance index that can be chosen to be the  $l_2$  or  $l_\infty$  norm,  $-\ln(\pi({\bf w}))$  is the probability cost, and the constant  $q^p \geq 0$  is the probability cost weight. The goal here is to minimize (17) subject to the system dynamics and constraints and the chance constraint. To find the optimal control input(s), the problem

equations must first be written in the mixed logical dynamical form. Then, the constrained optimization problem (i.e., the model predictive control problem) will be solved using mixed-integer programming (see [27] for details).

# III. DESCRIPTION OF THE SYSTEM EQUATIONS IN MIXED LOGICAL DYNAMICAL FORM

In this paper, the DHSA is first used to model the system, and then the system dynamics is represented in the MLD form. Finally, mixed-integer quadratic programming is employed to find the optimal control input. Fig. 2 presents the proposed controller design approach for CACC. As shown in the figure, CAVs leverage a look-ahead communication topology, and each CAV shares its predictive speed trajectory with a number of its followers. The DHSA unit is used to describe each CAV dynamics and constraints together with its five operating modes, namely free following (FF), warning (W), danger (D), emergency braking (E), and lane change (LC). In the control unit, the DHSA is transformed into MLD form and then used to solve the stochastic MPC problem. The optimal control input is applied to the system actuator(s), and the predictive speed trajectory is shared with follower vehicles through V2V communication. In the remainder of this section, some details about reformulating CAV equations in MLD form are presented.

The constraints on the system include bounds on the acceleration, input, road speed limit, and distance between vehicles (negative distance means collision and therefore, it should not occur). Therefore, the following inequalities should always hold true

$$a_i^{min} \le a_i(k) \le a_i^{max},\tag{18a}$$

$$u_i^{min} \le u_i^a(k) \le u_i^{max},\tag{18b}$$

$$v_i(k) \le v_{max},\tag{18c}$$

$$d_i(k) > 0. (18d)$$

As mentioned earlier, in our CACC design, the following five operating modes are considered with the transition diagram shown in Fig. 2:

- 1) free-following mode, where each CAV attempts to keep a desired distance from its CAV predecessors (see Figs. 3a 3f):
- 2) warning mode, where the adjacent HV may change its lane and move in front of a CAV (see Fig. 3b).
- danger mode, where an HV is changing (or has changed) its lane and is moving in front of the CAV (in this case, the CAV right behind the HV adjusts its headway according to the preceding HV's location (see Fig. 3d));
- 4) emergency-braking mode, where the CAV uses maximum feasible deceleration to avoid accident; e.g., in Fig. 3c, the orange CAV enters the emergency-braking mode to avoid possible crash into the black HV vehicle since the gap between the CAV and the HV is smaller than a safe distance:
- lane-change mode, in which the CAV tries to overtake an HV and reduces the distance between itself and its preceding CAVs (see Fig. 3e).

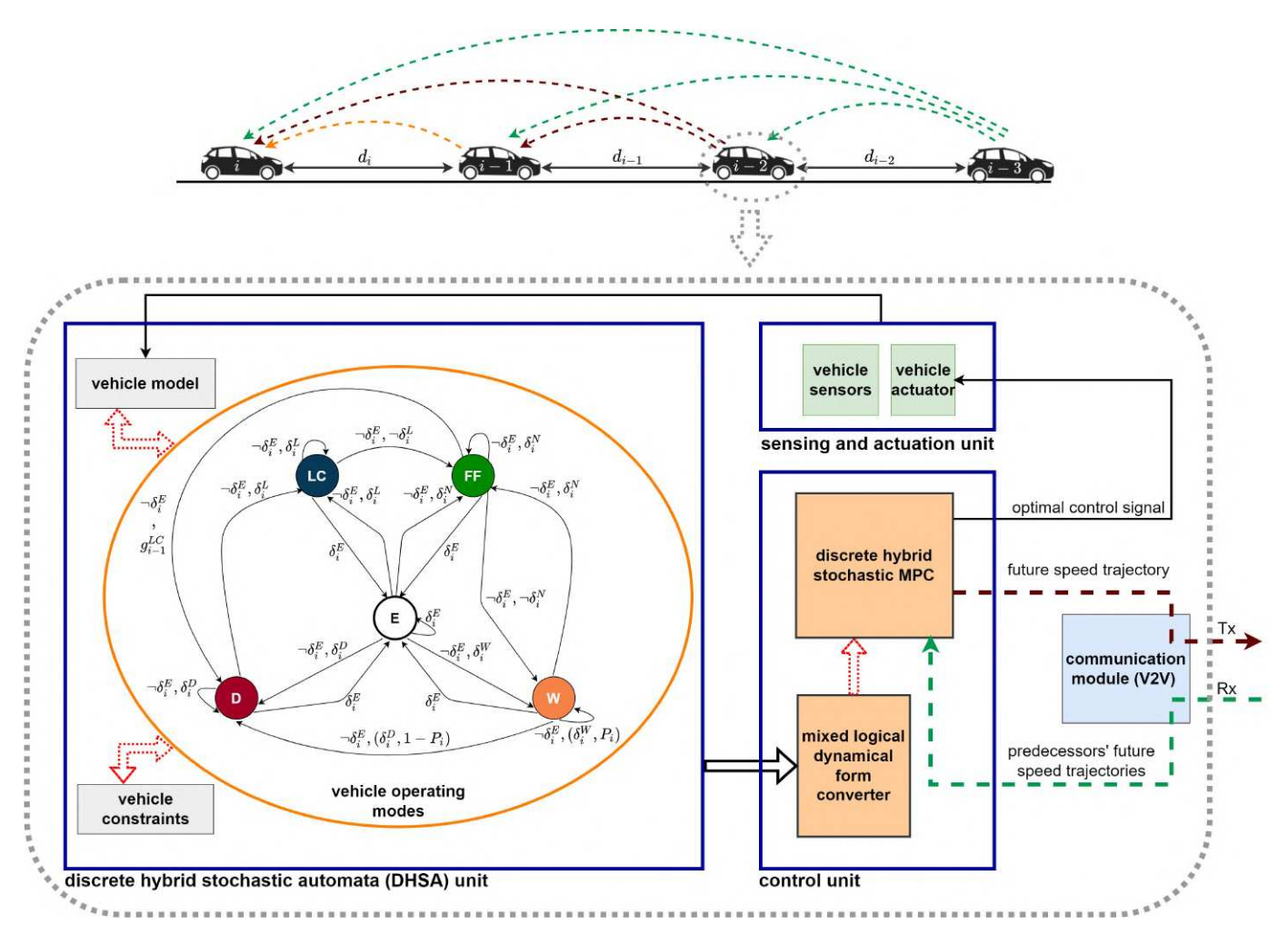


Fig. 2: Diagram of the proposed stochastic MPC design for CACC, in which each CAV's model including state-space equations, constraints, and operating modes (namely free following (FF), warning (W), danger (D), emergency braking (E), and lane change (LC)) is described using a DHSA. The control unit translates the DHSA into MLD and employs a discrete hybrid stochastic MPC to find the optimal control inputs. Each CAV uses the future speed profiles of its predecessors, which are received through V2V communication, for finding its optimal control actions.

Five binary auxiliary variables representing system event generators are defined as follows

$$\begin{split} \delta_i^N(k) &= 1 \iff \text{free-following event is activated;} \\ \delta_i^W(k) &= 1 \iff \text{warning event is activated;} \\ \delta_i^D(k) &= 1 \iff \text{danger event is activated;} \\ \delta_i^e(k) &= 1 \iff \text{emergency-braking event is activated;} \\ \delta_i^L(k) &= 1 \iff \text{lane-change event is activated.} \end{split}$$

The event generator functions are explained in detail in the rest of this section.

1) Emergency-braking Event: For safety and collision avoidance, the emergency-braking constraint is considered such that if  $\Delta d_i(k)$  goes below a fixed threshold  $(\underline{d}_i)$ ,  $i^{th}$  CAV should brake with the minimum possible acceleration  $(u_i^a(k) = u_i^{min})$ , thereby

$$\Delta d_i(k) + \underline{d}_i \le 0 \iff \delta_i^e(k) = 1. \tag{19}$$

The condition in (19) can be described in MLD form using the following inequalities

$$\Delta d_i(k) + \underline{d}_i \le M_i^e[1 - \delta_i^e(k)],$$
  

$$\Delta d_i(k) + d_i \ge \varepsilon + \delta_i^e(k)[m_i^e - \varepsilon],$$
(20)

where  $\varepsilon$  is the machine precision and and  $m_i^e$  and  $M_i^e$  are lower and upper bounds on  $\Delta d_i(k) + \underline{d}_i$ , respectively. To enforce hard braking, an upper bound constraint on  $u_i^a(k)$  is added such that

$$u_i^a(k) \le \delta_i^e(k) u_i^{min} + [1 - \delta_i^e(k)] u_i^{max}.$$
 (21)

As far as the system is operating in the free-following mode, the upper bound on acceleration input is  $u_i^{max}$ . However, when the emergency-braking mode is activated, the upper bound changes to  $u_i^{min}$ . We assume that reverse driving is not allowed and the speed cannot become negative. But the emergency-braking mode forces the input  $u_i^a(k) = u_i^{min}$  and the speed of the vehicle may become negative. To handle this issue, the constraint  $v_i(k) \geq 0$  is added to the system. However, this may result in contradictory constraints;  $v_i(k) \geq 0$ 

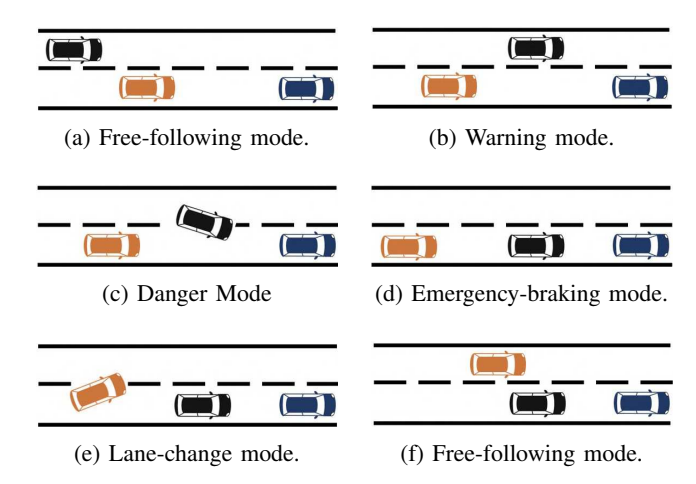


Fig. 3: Different operating modes for the CAV shown with orange color. The blue vehicle depicts the preceding CAV while the black vehicle represents the adjacent HV.

while  $v_i(k+1) = v_i(k) + t_s \, a_i(k)$  may become negative. To avoid this, two new auxiliary variables  $\delta_i^E(k)$  and  $f_i^1(k)$  are considered such that

$$v(k) \ge \underline{v}_i \iff f_i^1(k) = 1,$$
 
$$\delta_i^e(k) = 1 \text{ and } f_i^1(k) = 1 \iff \delta_i^E(k) = 1,$$
 (22)

and (21) is rewritten as

$$u_i^a(k) \le \delta_i^E(k) u_i^{min} + [1 - \delta_i^E(k)] u_i^{max}.$$
 (23)

Equation (23) implies that when the emergency-braking event is activated and  $v_i(k) > \underline{v}_i$ , then the control input should be set to its lowest value; otherwise, there is no need to enforce the vehicle's input to its minimum value. The statements in (22) are described in MLD form as

$$v_{i}(k) - \underline{v}_{i} \leq M_{i}^{v} f_{i}^{1}(k),$$

$$v_{i}(k) - \underline{v}_{i} \geq \varepsilon + [1 - f_{i}^{1}(k)](m_{i}^{v} - \varepsilon),$$

$$\delta_{i}^{E}(k) \geq \delta_{i}^{e}(k) + f_{i}^{1}(k) - 1,$$

$$\delta_{i}^{E}(k) \leq \delta_{i}^{e}(k),$$

$$\delta_{i}^{E}(k) \leq f_{i}^{1}(k),$$

$$(24)$$

where  $m_i^v$  and  $M_i^v$  are lower and upper bounds on  $v_i(k) - \underline{v}_i$ , respectively.

2) Warning and Danger Events: Warning event occurs whenever it is possible for an HV to change its lane and enter into the CAVs' platoon. For  $CAV_i$ , auxiliary variable  $g_i^W(k)$  is defined such that

$$x_i(k) + l_i^v \le x_i^h(k) \le x_{i-1}(k) - l_i^h \iff g_i^W(k) = 1, (25)$$

where  $x_i^h(k)$  and  $l_i^h$  denote the longitude and the length of the HV close to  $\mathrm{CAV}_i$ , respectively. If the HV passes the gap between two  $\mathrm{CAV}_i$  without switching its lane, the warning event terminates. Whenever the HV decides to switch the lane and moves in front of a CAV (which can be detected through the CAV sensors and cameras), danger event occurs. In this case, the CAV in danger mode should adjust its headway based on the HV position instead of the preceding CAV's position.

Remark 1: It is noted that the transition from warning mode to danger mode is a probabilistic event, which results from the unpredictable HV behavior. This probability can be estimated using the information received by CAV sensors. Since the estimation is beyond the scope of this paper, it is assumed that the CAV is aware of the transition probability. It is worth noting that in our problem, uncontrollable events  $(w_i(k))$  are the same as warning and danger event auxiliary variables  $(\delta_i^W(k))$  and  $\delta_i^D(k)$ .

To represent the occurrence of warning and danger events in MLD form, some inequalities are considered. Based on the aforementioned explanations, whenever  $g_i^W(k) = 1$ , either warning or danger event occurs, and hence

$$\delta_i^W(k) + \delta_i^D(k) = g_i^W(k). \tag{26}$$

Besides, if the danger event activates (meaning that the HV is entering/has entered into the CAVs' platoon), it remains active until the CAV switches its lane. Therefore

$$\delta_i^D(k) = 1 \text{ and } g_i^W(k) = 1 \to \delta_i^D(k+1) = 1.$$

This relation is shown in MLD form as follows

$$\delta_i^D(k) + g_i^W(k) - 1 - \delta_i^D(k+1) \le 0. \tag{27}$$

Danger event for  $CAV_i$  occurs for one of the following two reasons:

 a) the CAV is in warning mode, and the adjacent HV begins changing its lane and entering the CAVs' platoon. In this case, the following statement should hold true

$$\delta_i^D(k-1)=0 \ \ \text{and} \ \ \delta_i^D(k)=1 \rightarrow \delta_i^W(k-1)=1,$$

which means that danger event cannot be activated unless the warning event is activated first. The aforementioned relation turns into the following inequalities in the MLD form

$$\delta_i^D(k) - \delta_i^D(k-1) - \delta_i^W(k-1) \le 0.$$
 (28)

b)  $CAV_i$  is in the free-following mode, and  $CAV_{i-1}$  is doing a lane change; hence, the  $i^{th}$  CAV's immediate predecessor in the lane becomes an HV. In this case,  $CAV_{i-1}$  announces its lane-change decision as a binary flag (shown as  $g_{i-1}^{LC}$  in the transition diagram in Fig. 2) to its follower CAV through communication. Hence, the following statement should hold true

$$g_{i-1}^{LC}(t) = 1 \to \delta_i^D(t) = 1.$$

As shown in Fig. 2, if each of four events, including free-following, warning, danger, and lane change occurs while emergency-braking event is **not** activated, vehicle mode switches based on the current activated event. However, due to the importance of emergency braking for preserving safety, this operating mode has priority over the other operating modes.

Remark 2: When the danger event occurs, the CAV adjusts its velocity and headway based on the HV that causes the danger. Hence, the CAV's distance from its preceding vehicle

(which can be either a CAV or an HV)  $d_i(k)$  can be redefined as

$$d_i(k) = \left(1 - \delta_i^D(k)\right) x_{i-1}(k) + \delta_i^D(k) \, x_i^h(k) - x_i(k) - l_i^v,$$
 and  $\Delta d_i(k)$  changes accordingly.

3) Lane-change Event: CAVs may require a lane change to achieve their desired spacing from their predecessors after an HV enters into the CAV platoon. Hence, when a CAV is in danger mode, and its longitudinal distance from its preceding CAV exceeds a predefined threshold (e.g., the threshold can be related to the fixed time gap), the CAV should perform a lane change to be able to accelerate and reach its desired spacing policy; in other words,

$$\delta_i^L(k) = 1 \iff x_{i-1}(k) - x_i(k) - l_i^v - (T_i + \alpha_i) v_i(k) > 0,$$

where  $\alpha_i > 0$  is the threshold mentioned above. Whenever the lane-change mode activates, the lateral reference for the CAV changes to the desired lateral location in the adjacent lane.

To assure a collision-free lane change, CAVs should also consider HVs in the target lane (e.g., in Fig. 3a, if the orange CAV decides to perform a lane change, it should also take the location and velocity of the black HV into account to avoid possible collision). To this aim, the lane-change mode for a CAV should not activate unless there is no vehicle in the target lane behind the CAV or the CAV is able to preserve a minimum distance from that vehicle during the lane-change maneuver; the latter for  $CAV_i$  is addressed using the following constraint

$$x_i(k) - x_{i+1}^h(k) - l_{i+1}^h(k) - \beta_i v_{i+1}^h \ge 0,$$

where  $\beta_i$  represents the minimum allowed time gap from the rear HV in the target lane,  $x_{i+1}^h$ ,  $l_{i+1}^h$  and  $v_{i+1}^h$  are location, length, and velocity of the HV in the CAV's target lane, respectively. It is noted that whenever the lane-change mode activates for  $CAV_i$ , danger event for that vehicle terminates.

4) Free-following Event: Free-following event for  $i^{th}$  CAV occurs when none of the surrounding HVs are able to enter the CAVs fleet right in front of  $CAV_i$ .

Considering the aforementioned events changes the difference equations in (8) to the following form

$$x_{i}(k+1) = (I + t_{s} A_{i}) x_{i}(k) + t_{s} B_{i} u_{i}(k) + t_{s} C_{i} [(1 - \delta_{i}^{D}(k)) v_{i-1}(k) + \delta_{i}^{D}(k) v_{i}^{h}(k)], \quad (29)$$

where  $v_i^h(k)$  is the velocity of the HV that activates danger event for  $i^{th}$  CAV.

For the defined problem, chance constraint is built based on two stochastic events (HV does not switch lane with probability  $P_i(k)$  and HV switches lane with probability  $1 - P_i(k)$ ). Consequently, the following constraint is considered

$$\sum_{k=1}^{N} \delta_{i}^{W}(k) \ln(P_{i}(k)) + g_{i}^{D}(k) \ln(1 - P_{i}(k)) \ge \ln(\tilde{P}_{i}),$$

where 
$$\delta_i^D(k) = 1$$
 and  $\delta_i^D(k-1) = 0 \iff g_i^D(k) = 1$ .

The new auxiliary variable  $g_i^D(k)$  is defined to detect when danger event activates (which is a probabilistic event). In the

former equation,  $\tilde{P}_i$  is chosen such that the trajectories with small probability are discarded.

#### IV. DISCRETE HYBRID STOCHASTIC MPC DESIGN

To achieve a stable CACC design, the goal is that the distance between CAVs converges to its desired value while vehicles move with equal and constant speed. MPC has shown to have the capability of controlling multi-input multi-output systems. However, for the CACC problem, when the number of vehicles increases, centralized MPC is not time-efficient [18]. Instead, distributed MPC can be used to reach a string stable CACC. The MPC problem for  $CAV_i$ , which employs an m-vehicle-ahead communication topology, at time t is defined as follows

$$\min_{\mathbf{u}_{i},\mathbf{w}_{i},\mathbf{z}_{i}} \sum_{k=0}^{N-1} \left[ (x_{i}(k) - R_{i})^{T} Q_{i} (x_{i}(k) - R_{i}) - q_{i}^{p} \left[ \delta_{i}^{W}(k) \ln(P_{i}) + g_{i}^{D}(k) \ln(1 - P_{i}) \right] + \sum_{j=i-m}^{i-1} \left[ c_{i,j}^{d} \left( x_{j}(k) - x_{i}(k) - \sum_{r=j+1}^{i} (d_{r}^{*}(k) + l_{r}^{v}) \right)^{2} + c_{i,j}^{v} \left( v_{j}(k) - v_{i}(k) \right)^{2} \right] + c_{i}^{E} \delta_{i}^{E}(k) ,$$
(31)

subject to : system equations in MLD form, chance constraints,

where  $\mathbf{u}_i$ ,  $\mathbf{z}_i$  and  $\mathbf{w}_i$  are the system inputs, the vector of auxiliary variables, and stochastic events, from k=0 to k=N-1, respectively. The constant  $q_i^p$  is the probability cost weight,  $c_{i,j}^d > 0$  and  $c_{i,j}^v$  are positive coefficients penalizing the distance and speed difference between  $CAV_i$  and  $CAV_j$  (j < i),  $c_i^E > 0$  penalizes the occurrence of emergency braking, and m denotes the number of predecessors sharing information with the  $i^{th}$  CAV. In (31), each vehicle tends to achieve the desired distances from its m predecessors while adjusting its velocity based on the predecessors' velocity. It is noted that when m > i (the number of predecessors is less than m),  $CAV_i$  replaces m with i in (31).

Each CAV sends its current speed information, and current and predicted acceleration information every  $t_c$  seconds. To avoid unnecessary data exchange, it is assumed that  $t_c \geq t_s$ . Therefore, each vehicle uses last received data to solve (31) until the preceding vehicle shares new information. Hence, each vehicle solves its MPC problem every  $t_s$  seconds and finds  $\mathbf{u}_i^*(k)$ ,  $\mathbf{x}_i^*(k)$ , and  $\mathbf{w}_i^*(k)$ . Then, it discards  $\mathbf{w}_i^*(k)$  and applies  $\mathbf{u}_i^*(0)$  to the system. Fig. 2 summarizes the details of the proposed control scheme.

Remark 3: When a CAV enters warning mode, its predictive trajectory can be affected by the probability cost weight and the chance constraint. When  $q_i^p$  is relatively large, the CAV's behavior may become conservative, meaning that it may predict that the HV would perform a lane change in the near future (within the prediction horizon) thus increasing its headway to avoid the possible danger.

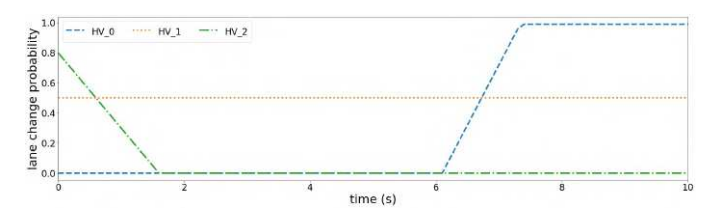


Fig. 4: The CAVs' estimation of the HVs' lane-change probabilities in the first 10 seconds of the simulation. It is assumed that the estimated probabilities remain the same for the remainder of the simulation.

#### V. SIMULATION RESULTS

For the CACC problem, the performance of the proposed hybrid and stochastic MPC scheme in a mixed-autonomy traffic system including two lanes, where HVs may perform lane change and merge into the CAVs' platoon, is evaluated. Parameters used in the simulation study are given in Table I. Assuming that CAVs use a four predecessor-following communication scheme  $(m=4),\ Q_i,\ c_{i,j}^d,\$ and  $c_{i,j}^v$  used in the simulation studies are considered as follows

$$\begin{split} Q_i &= \mathrm{diag}[2.5 \ 1 \ 1 \ 1], \\ c^d_{i,i-1} &= 3.5, \quad c^v_{i,i-1} = 0.88, \\ c^d_{i,i-2} &= 2.5, \quad c^v_{i,i-2} = 0.63, \\ c^d_{i,i-3} &= 1.25, \quad c^v_{i,i-3} = 0.31, \\ c^d_{i,i-4} &= 0.83, \quad c^v_{i,i-4} = 0.21. \end{split}$$

In the MPC problem in (31), the vector  $R_i$  is chosen as follows

$$\begin{split} R_i &= \left[ 0.7 \, \delta_i^D(k) \, T_i \, v_i(0) \quad \quad 0 \quad \quad y_i^{ref}(k) \\ & \left( 1 - \delta_i^D(k) \right) v_{i-1}(k) - \delta_i^D(k) \, v_i^h(k) \quad \quad 0 \right]^T. \end{split}$$

Such selection for  $R_i$  implies that if danger event does not occur (or will not occur within the prediction horizon),  $CAV_i$  only considers its m predecessor CAVs' information for adjusting its speed. However, according to Remark 2, the activation of danger event results in taking the distance from the adjacent HV and the HV's velocity into account in finding the optimal control input. It is noted that  $CAV_i$  uses  $T_i(v_i(k) + 0.7 v_i(0)) + d_i^0$  as its desired distance from the adjacent HV in danger mode. The underlying mixed-integer optimization problems are solved using CVXPY package, and Gurobi solver in Python [29]-[31]. It is noted that the average computational time to solve the mixed-integer programming problem, i.e., (31), using an 11th generation Intel-R Core<sup>TM</sup> i7-11800H @ 2.30GHz laptop is under 5 ms. As mentioned earlier in Remark 1, it is assumed that CAVs have an estimation of the HVs' lane-change probability, as shown in Fig. 4. It is also assumed that HVs may perform lane change only once during the simulation study. Two sets of experiments are conducted; in the first one, performance of the proposed controller is evaluated in a mixed-autonomy environment, including seven CAVs and three HVs. In the second experiment, our proposed stochastic MPC approach is compared against a switching controller, whose structure design is described later in this section.

TABLE I: Model and optimization parameters used in the simulation studies.

parameter	value	parameter	value
$t_s$	0.1  s	m	4
$T_i$	0.7s	$ au_i$	0.1 s
$l_i^v$	5 m	$l_i^h$	5 m
$\underline{d}_i$	2m	$d_i^0$	2 m
$a_i^{min}$	$-4  m/s^2$	$a_i^{max}$	$3 m/s^2$
$u_i^{min}$	$-4  m/s^2$	$u_i^{max}$	$4 m/s^2$
$q_i^p, i = 1, 5$	2000	$q_i^p,  \forall  i \neq 1, 5$	1
$v_{max}$	35m/s	$\underline{v}_i$	1  m/s
N	7	$\beta_i$	0.3s
$\hat{P}_i$	$0.01^{N}$	$c_i^E$	100

#### A. Evaluation of the Proposed Controller Performance

In our first set of experiments, where a mixed-autonomy environment is studied, a platoon of seven CAVs is considered while three HVs are assumed to move initially in the adjacent lane next to the CAVs. The subplots showing  $\Delta d_i$ ,  $y_i$ ,  $v_i$ ,  $a_i$ , and  $\delta_i^E$  are given in Fig. 5 while the graphical representation of the simulation at eight different moments is illustrated in Fig. 6. The location of the vehicles at the beginning of the simulation is shown in the first subplot. Initially, the velocity of both  $HV_0$  and  $HV_1$  is 26 m/s while the velocity of  $HV_2$ is  $20 \, m/s$ .  $HV_0$  performs a lane change at  $t = 9 \, s$  while keeping the same speed. However, when  $HV_1$  changes its lane at t = 12 s, it also reduces its speed to 23 m/s.  $HV_3$  does not perform a lane change. The initial velocity for all CAVs is  $20 \, m/s$  while their desired velocity is  $29 \, m/s$ . For better readability, the discussion about simulation results focuses on eight critical time instants as presented in Fig. 6.

1) At t = 0s: At the beginning of the simulation, the first, second, fourth, and sixth CAVs operate in free-following mode, while  $CAV_3$  and  $CAV_5$  are in the warning mode. According to Remark 3,  $CAV_5$  behaves conservatively (since  $q_5^p = 2000$  is relatively large) and expects that the HV would perform a lane change within the prediction horizon, thereby entering the danger mode. Hence,  $CAV_5$  increases its distance from the preceding CAV to accommodate the possible HV's lane change (as shown in the first subplot in Fig. 5,  $\Delta d_5$  noticeably increases at the beginning). After around one second, its prediction about the future mode changes as its estimation of  $HV_2$  lane-change probability changes (as shown in Fig. 4, the estimated lane-change probability decreases over time), and it adjusts its headway based on its desired spacing policy  $d_5^*$ . The CAVs' headway and velocity converge to their desired value at around t = 7 s.

2) At t=9.3s: Based on the estimated lane-change probability for  $HV_0$  and relatively large value for probability cost weight  $q_1^p=2000$ ,  $CAV_1$  expects that  $HV_0$  performs a lane change.  $HV_0$  finally decides to switch its lane and merge into the platoon at  $t=9\,s$ . The aforementioned lane change causes  $CAV_1$  operating mode to change from warning to danger. However, since  $CAV_1$  expected such maneuver, it

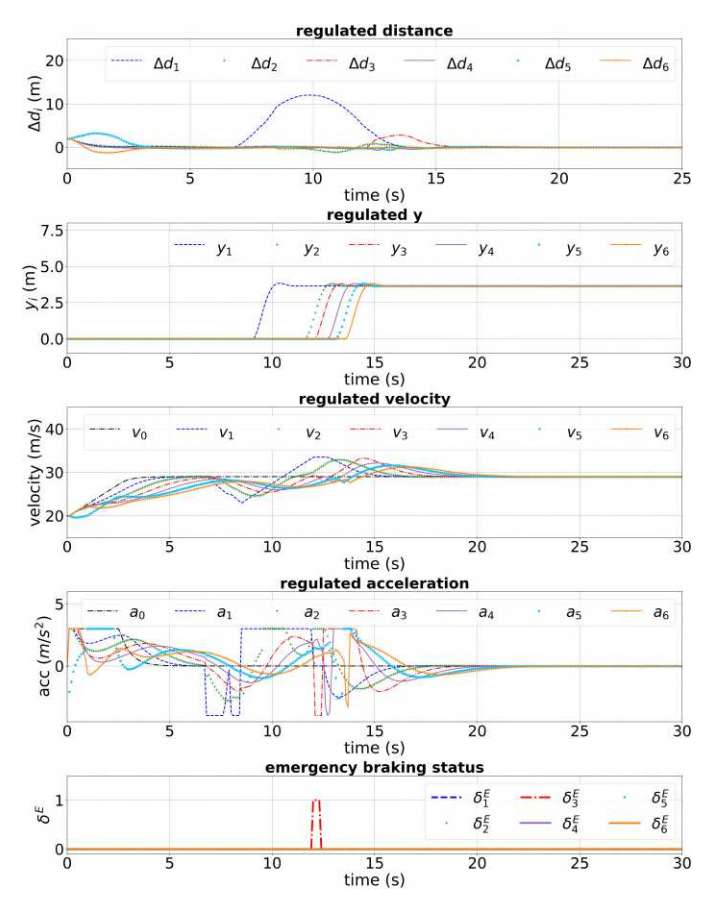


Fig. 5: Performance of the CAVs employing the proposed control scheme for a scenario including seven CAVs and three HVs when the lane-change event threshold is  $\alpha_i=0.25\,s$  (corresponding to the graphical representation in Fig. 6). From top to bottom, the first subplot depicts  $\Delta d_i$ ; the second subplot shows each vehicle's lateral location; velocity and acceleration are shown in the third and fourth subplot, respectively; the last subplot illustrates the emergency-braking status for each vehicle.

has already increased its distance from its preceding CAV to accommodate the HV's lane change, and the HV safely switches its lane. Later at around  $t=9.3\,s,\,CAV_1$  enters lane-change mode and decides to enter the left lane and to avoid its distance from the leader going beyond the predefined threshold ( $\alpha_i=0.25\,s$ ). It is noted that when the lane change is completed, the corresponding CAV enters the free-following mode.

- 3) At t=11.7s: As the first CAV changes its lane,  $CAV_2$  immediate predecessor in its lane becomes an HV; hence, the second CAV also enters the danger mode and takes its distance from the HV into account for adjusting its headway.  $CAV_2$  waits until  $t=11.7\,s$  to be able to safely change its lane and keep its distance from the preceding CAVs close to the desired value. Second CAV lane-change maneuver forces  $CAV_3$  to enter the danger mode because its predecessor becomes an HV.
- 4) At t = 12.3s:  $CAV_3$  assumes that the adjacent HV in the left lane will not switch its lane. Despite the third CAV's

- assumption,  $HV_1$  suddenly decides to merge into the CAVs' platoon at  $t=12\,s$ . This maneuver forces  $CAV_3$  to enter the danger mode. Due to the small distance between the CAV and the HV,  $CAV_3$  enters the emergency mode for about  $0.3\,s$  (see the last subplot in Fig. 5). Then, the controller's optimal decision is to perform a lane change to bypass the HV and keep  $CAV_3$  close to the preceding CAVs.
- 5) At t=13s: As the third CAV changes its lane,  $CAV_4$  immediate predecessor in its lane becomes an HV; hence the fourth CAV also enters the danger mode and takes its distance from the HV into account for adjusting its headway. A few moment later, at  $t=13\,s$ ,  $CAV_4$  makes the same decision as its preceding CAV and switches to lane-change mode.
- 6) At t = 13.5s: Similar to  $CAV_4$ ,  $CAV_5$  performs a lane change at t = 13.5s to keep  $\Delta d_5$  close to zero.
- 7) At t = 13.8s:  $CAV_6$  also reacts to its predecessor's lane change quickly by performing a lane change at t = 13.8 s to keep  $\Delta d_6$  close to zero.
- 8) At t=20s: A few seconds after all follower CAVs changed their lane, all follower vehicles operate in free-following mode in the left lane, and their velocity and spacing policy converges to their desired values (see Fig. 5).

It is noted that according to Fig. 5, the proposed control scheme is able to preserve string stability as the deviations from the desired spacing policy do not propagate in the platoon. As mentioned earlier, there exists a number of deviations from the desired spacing policy, as well as the desired velocity in Fig. 5, which are resulted from the lane change performed by HVs. Furthermore, the duration and the peak of those deviations increase as the threshold for lane-change event  $(\alpha_i)$  increases since with larger  $\alpha_i$ , CAVs will wait longer before they perform a lane-change maneuver to compensate for the increased distance from their preceding CAVs. For better illustration, a simulation for the same scenario is conducted using  $\alpha_i = 0.4 \, s$ . Results shown in Fig. 7 confirm the aforementioned statement.

## B. Comparison of the Proposed Design Approach Against a Switching Control

The performance of the proposed stochastic hybrid MPC design method is compared against a switching controller whose structure is shown in Fig. 8. The decision-making unit chooses the proper controller such that (based on the definitions of different CAV operating modes in section III) if the CAV is in free following mode, the FF-MPC is engaged; if CAV enters the danger mode, Danger-MPC is activated; whenever emergency braking condition is violated, EB-Controller is engaged; finally, when the distance between two successive CAVs increases, Lateral-MPC is used. A scenario including three CAVs and one HV is considered with the graphical representation shown in Fig. 9. Results for the stochastic MPC are shown in Fig. 9a while the results for the switching controller are depicted in Fig. 9b. The location of the vehicles at the beginning of the simulation is shown in the first subplots (t = 0 s). Initially, the velocity of the HV is 29 m/s. It accelerates at t = 10 s to reach 32 m/s, then at t = 17 sit reduces its speed to  $29 \, m/s$ . Finally, it performs a lane

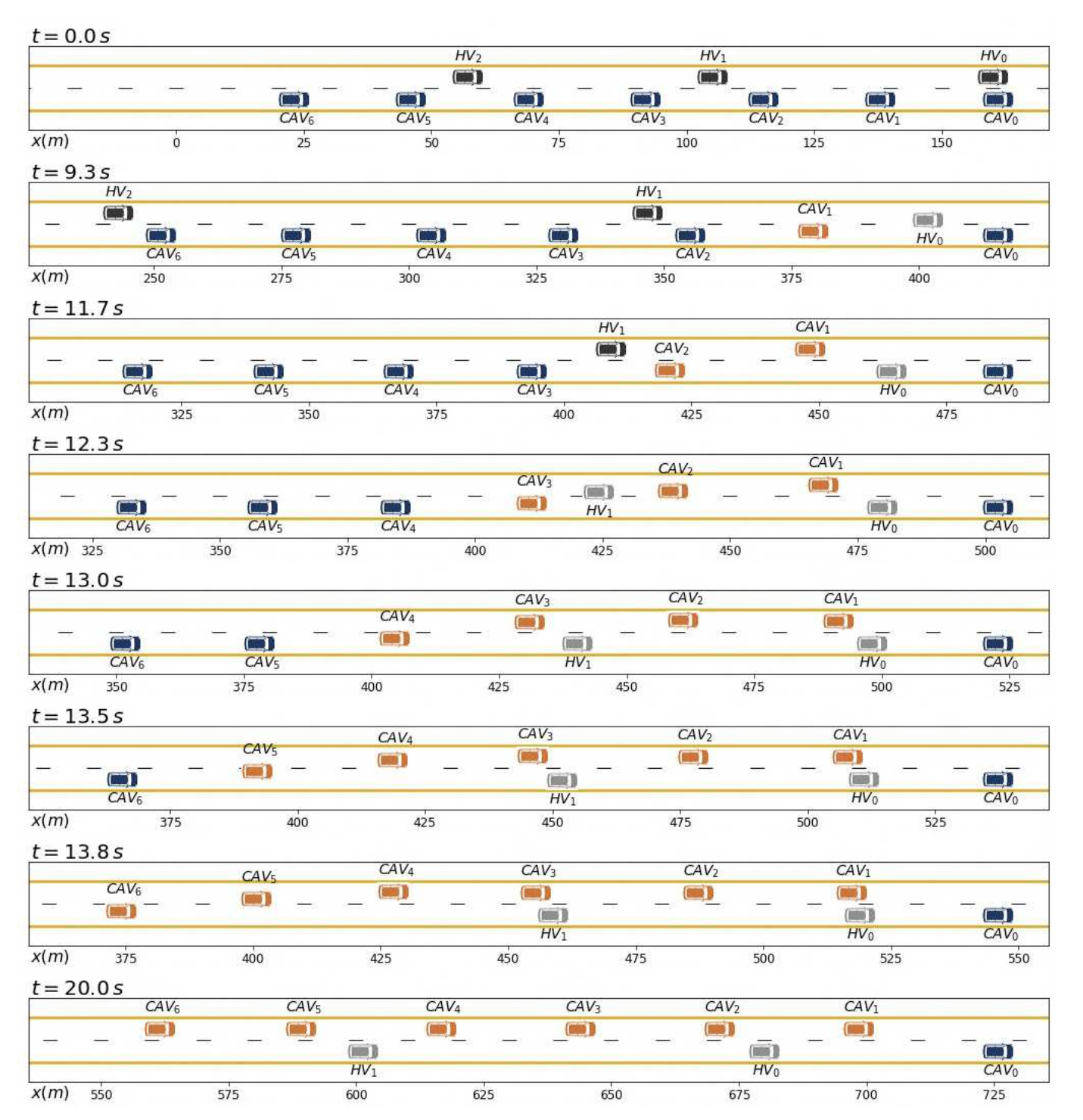


Fig. 6: The graphical representation of the simulation study for a scenario including seven CAVs and three HVs where  $\alpha_i=0.25\,s$ . HVs in the top lane are shown in black, while after beginning a lane change, their color is changed to gray. CAVs are shown using blue color, and after their lane-change mode activates, their color is changed to orange. At  $t=0\,s$ , three HVs are in the top lane, and all the AVs are in the bottom lane. As  $CAV_1$  expects, at  $t=9.3\,s$ ,  $HV_0$  performs a lane change to merge into the CAVs' platoon. Meanwhile,  $CAV_1$  observes the HV's lane change and the controller detects that its distance from its preceding CAV would exceed the predefined threshold; hence, it switches its lane to bypass the HV and achieve its desired distance from its predecessor CAV.  $CAV_2$  waits until  $t=11.7\,s$  to safely change its lane and keep its distance from the preceding CAV close to the desired value. After a few seconds,  $HV_1$  suddenly decides to merge into the CAVs' platoon at  $t=12\,s$  while  $CAV_3$  does not expect that behavior to increase the gap in front of it. Hence, it briefly enters the emergency-braking mode and then changes its lane.  $CAV_4$  decides to switch to the top lane to avoid increasing its distance from its predecessor CAV at  $t=13\,s$ . Shortly after, at  $t=13.5\,s$ ,  $CAV_5$  does the same thing. At  $t=13.8\,s$ , the last CAV in the platoon also changes its lane to keep its desired distance from its predecessor CAVs, and at  $t=20\,s$ , all follower CAVs are in the top lane and successfully able to achieve their desired velocity and spacing policy.

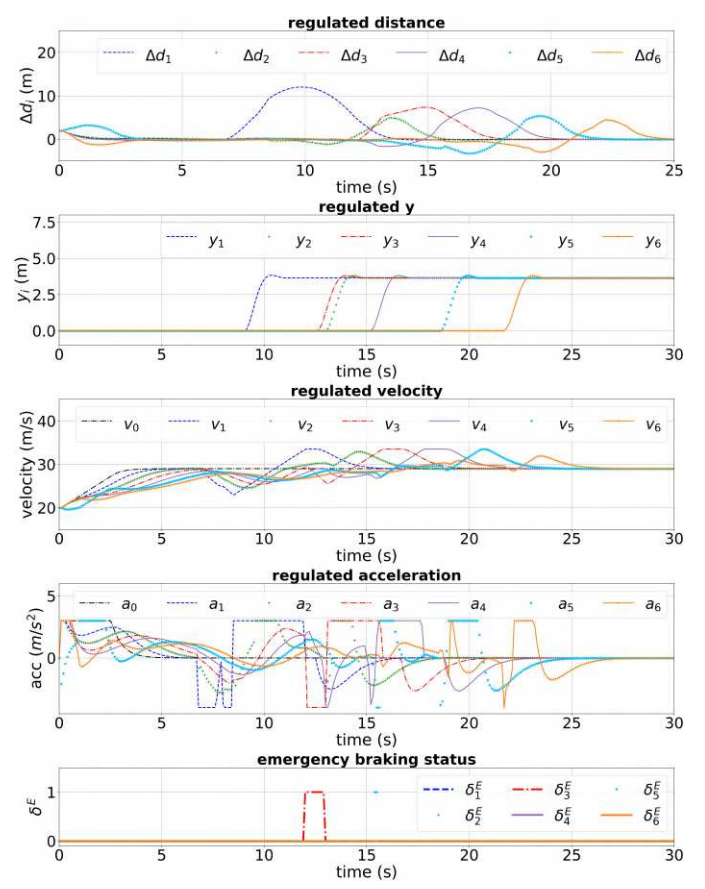


Fig. 7: Performance of the CAVs employing the proposed controller for a scenario including seven CAVs and three HVs when the threshold for lane-change event is  $\alpha_i = 0.4 \, s$ . Larger values for  $\alpha_i$  delay the CAVs' lane-change process, resulting in more fluctuations in  $\Delta d_i$ , while the desired case is to keep  $\Delta d_i$  close to zero.

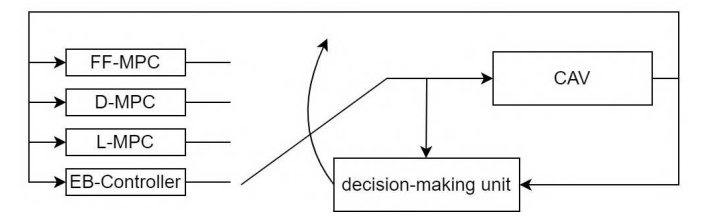


Fig. 8: Diagram of the switching control approach. The decision-making unit chooses the proper controller among the four available options, namely free-following MPC (FF-MPC), danger-MPC (D-MPC), lateral-MPC (L-MPC), and emergency-braking controller (EB-Controller).

change at  $t=19\,s$  while reducing its speed to  $27\,m/s$ . The initial velocity for all CAVs is  $20\,m/s$  while their desired velocity is  $29\,m/s$ . For a better readability, the discussion about simulation results focuses on five time instants as presented in Fig. 9. It is noted that for the stochastic MPC,  $q_1^p=q_2^p=2,000$  is considered.

1) At t=0 s: At the beginning of the simulation, for the stochastic MPC (Fig. 9a), all CAVs operate in free-following mode. The decision-making unit for all CAVs for the switching

control chooses FF-MPC at this moment.

2) At t=10 s: According to Remark 3,  $CAV_2$  behaves conservatively (since  $q_2^p=2,000$  is relatively large) and expects that the HV would perform a lane change within the prediction horizon, thereby entering the danger mode. Hence,  $CAV_2$  increases its distance from the preceding CAV to accommodate the possible HV's lane change. However, there is no change in the decision of the switching control compared to t=0 s. At this moment, the HV accelerates to pass  $CAV_1$  and possibly changes its lane afterward.

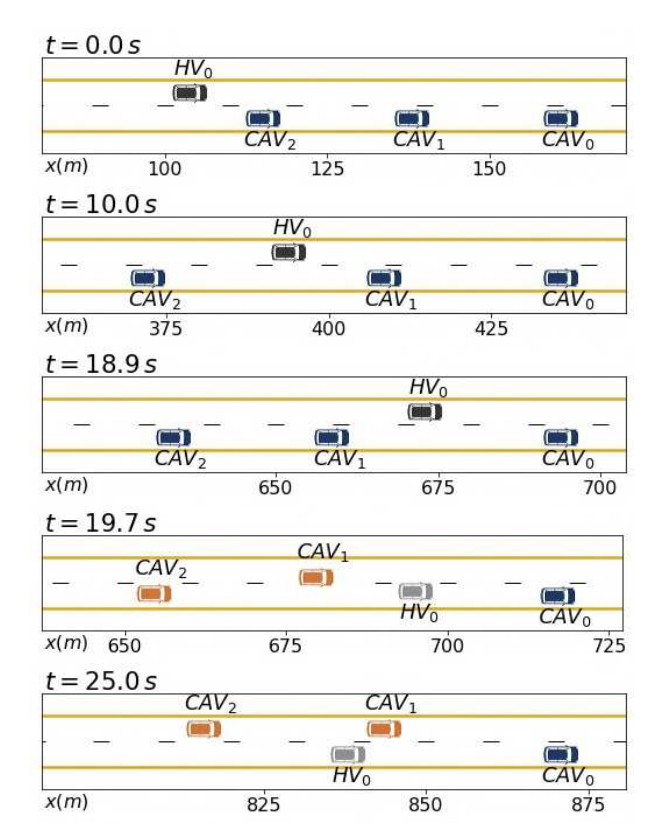
3) At t=18.9~s: The stochastic MPC for  $CAV_1$  decides to increase the CAV's headway to accommodate the HV's possible lane change (Fig. 9a). However, the switching control approach does not make a new action and operates the same as the previous steps (e.g., t=10~s). It is noted that the longitudinal distance between  $CAV_1$  and the HV for the stochastic MPC is noticeably larger than the switching control method at this moment.

4) At  $t=19.7\ s$ : As shown in Fig. 9, at  $t=19.7\ s$ , the HV performs a lane change, and both controllers decide that  $CAV_1$  should perform a lane-change maneuver in response to the HV's behavior. However, there is a noticeable difference in the lane change maneuver when comparing the two controllers. While the stochastic MPC performs a safe lane-change maneuver with an acceptable headway from the HV, in the switching control method,  $CAV_1$  crosses the lane with only a few centimeters distance from the HV, which is a near-accident case thereby violating safety standards (e.g., maintaining a minimum required headway).

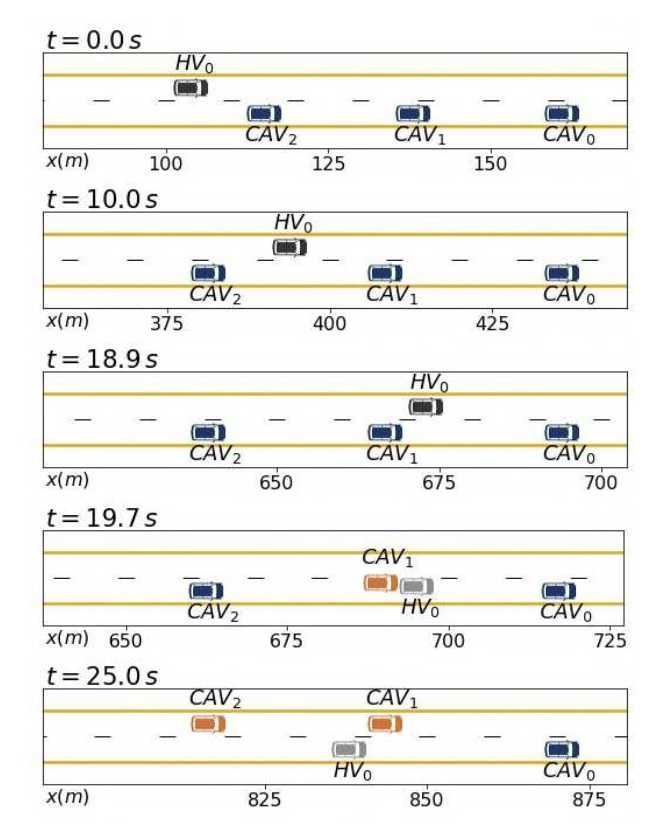
5) At  $t=25\ s$ : A few seconds after both follower CAVs changed their lane, their velocity and spacing policy converges to their desired values, resulting in similar performance for both controllers.

#### VI. CONCLUSION

In this paper, a stochastic MPC design method has been developed based on a discrete hybrid stochastic model for CACC applications aiming at safe and efficient platooning in a mixedautonomy traffic environment. It is assumed that each CAV can measure distance from its immediate predecessor, as well as the predecessor's velocity. It is also assumed to have access, through communication, to a limited number of predecessors' locations, speed, and predictive speed profile. Since vehicles do not need other vehicles' models, the proposed MPC design method can be applied to a heterogeneous fleet of vehicles in the platoon. The proposed MPC scheme integrates five operating modes for each vehicle: free following, warning, danger, emergency braking, and lane change, to adapt the CAV's behavior based on the HVs maneuvers. Each CAV's operating mode is chosen based on the predictive information it receives from its predecessors and the estimated behavior of surrounding HVs. Introducing free-following and emergencybraking modes leads to an efficient and safe autonomous driving. Switching between warning, danger, and lane-change modes maintains the platoon's behavior close to the desired performance during unexpected human-driven vehicle maneuvers. The proposed stochastic controller is also shown to



(a) Performance of the proposed stochastic MPC approach for the second scenario. Although the proposed MPC method may result in unnecessary maneuvers (e.g.,  $CAV_2$  temporarily increases its headway to make room for a possible HV lane-change maneuver that did not occur), its predictive behavior and reactions based on stochastic mode transition preserve safety for  $CAV_1$ .



(b) Performance of the switching control approach for the second scenario. In this case,  $CAV_2$  does not make any extra maneuver while the HV moves in the adjacent lane. However, this control approach can barely preserve safety during the HV's lane-change maneuver as  $CAV_1$  longitudinal distance from the HV is a few centimeters since this approach does not react based on stochastic events.

Fig. 9: The graphical representation of the simulation study for the second scenario including three CAVs and one HV where  $\alpha_i = 0.25 \, s$ .

successfully counteract the effect of sudden HV maneuvers and lane change by providing a smooth acceleration profile. The comparison between the performance of the proposed stochastic MPC and a switching control further illustrates the benefits of the proposed approach.

#### REFERENCES

- [1] T. Peng, L. Su, R. Zhang, Z. Guan, H. Zhao, Z. Qiu, C. Zong, and H. Xu, "A new safe lane-change trajectory model and collision avoidance control method for automatic driving vehicles," *Expert Systems with Applications*, vol. 141, p. 112953, 2020.
- [2] A. Vahidi and A. Eskandarian, "Research advances in intelligent collision avoidance and adaptive cruise control," *IEEE transactions on intelligent transportation systems*, vol. 4, no. 3, pp. 143–153, 2003.
- [3] J. Ni, J. Han, and F. Dong, "Multivehicle cooperative lane change control strategy for intelligent connected vehicle," *Journal of Advanced Transportation*, vol. 2020, 2020.
- [4] Z. Zhang, L. Zhang, J. Deng, M. Wang, Z. Wang, and D. Cao, "An enabling trajectory planning scheme for lane change collision avoidance on highways," *IEEE Transactions on Intelligent Vehicles*, 2021.
- [5] M. Wang, S. P. Hoogendoorn, W. Daamen, B. van Arem, and R. Happee, "Game theoretic approach for predictive lane-changing and car-following control," *Transportation Research Part C: Emerging Technologies*, vol. 58, pp. 73–92, 2015.
- [6] C. Wang, Q. Sun, Z. Li, and H. Zhang, "Human-like lane change decision model for autonomous vehicles that considers the risk perception of drivers in mixed traffic," *Sensors*, vol. 20, no. 8, p. 2259, 2020.

- [7] I. Papadimitriou and M. Tomizuka, "Fast lane changing computations using polynomials," in *Proceedings of the 2003 American Control Conference*, 2003., vol. 1, pp. 48–53, IEEE, 2003.
- [8] Y. Luo, Y. Xiang, K. Cao, and K. Li, "A dynamic automated lane change maneuver based on vehicle-to-vehicle communication," *Transportation Research Part C: Emerging Technologies*, vol. 62, pp. 87–102, 2016.
- [9] S. Liu, H. Su, Y. Zhao, K. Zeng, and K. Zheng, "Lane change scheduling for autonomous vehicle: A prediction-and-search framework," in Proceedings of the 27th ACM SIGKDD Conference on Knowledge Discovery & Data Mining, pp. 3343–3353, 2021.
- [10] W. Cao, M. Mukai, T. Kawabe, H. Nishira, and N. Fujiki, "Cooperative vehicle path generation during merging using model predictive control with real-time optimization," *Control Engineering Practice*, vol. 34, pp. 98–105, 2015.
- [11] C. Menendez-Romero, M. Sezer, F. Winkler, C. Dornhege, and W. Burgard, "Courtesy behavior for highly automated vehicles on highway interchanges," in 2018 IEEE Intelligent Vehicles Symposium (IV), pp. 943–948, IEEE, 2018.
- [12] J. Guanetti, Y. Kim, and F. Borrelli, "Control of connected and automated vehicles: State of the art and future challenges," *Annual reviews* in control, vol. 45, pp. 18–40, 2018.
- [13] B. Van Arem, C. J. Van Driel, and R. Visser, "The impact of cooperative adaptive cruise control on traffic-flow characteristics," *IEEE Transac*tions on intelligent transportation systems, vol. 7, no. 4, pp. 429–436, 2006.
- [14] F. Morbidi, P. Colaneri, and T. Stanger, "Decentralized optimal control of a car platoon with guaranteed string stability," in *2013 European Control Conference (ECC)*, pp. 3494–3499, IEEE, 2013.

- [15] J. Ploeg, "Analysis and design of controllers for cooperative and automated driving," 2014.
- [16] G. Guo and W. Yue, "Sampled-data cooperative adaptive cruise control of vehicles with sensor failures," *IEEE Transactions on Intelligent Transportation Systems*, vol. 15, no. 6, pp. 2404–2418, 2014.
- [17] H. Xing, J. Ploeg, and H. Nijmeijer, "Compensation of communication delays in a cooperative acc system," *IEEE Transactions on Vehicular Technology*, vol. 69, no. 2, pp. 1177–1189, 2019.
- [18] Y. Zhou, M. Wang, and S. Ahn, "Distributed model predictive control approach for cooperative car-following with guaranteed local and string stability," *Transportation research part B: methodological*, vol. 128, pp. 69–86, 2019.
- [19] C. Zhai, Y. Liu, and F. Luo, "A switched control strategy of heterogeneous vehicle platoon for multiple objectives with state constraints," *IEEE Transactions on Intelligent Transportation Systems*, vol. 20, no. 5, pp. 1883–1896, 2018.
- [20] R. Kianfar, P. Falcone, and J. Fredriksson, "A control matching model predictive control approach to string stable vehicle platooning," *Control Engineering Practice*, vol. 45, pp. 163–173, 2015.
- [21] Z. Wang, G. Wu, and M. J. Barth, "A review on cooperative adaptive cruise control (cacc) systems: Architectures, controls, and applications," in 2018 21st International Conference on Intelligent Transportation Systems (ITSC), pp. 2884–2891, IEEE, 2018.
- [22] R. Pueboobpaphan, F. Liu, and B. van Arem, "The impacts of a communication based merging assistant on traffic flows of manual and equipped vehicles at an on-ramp using traffic flow simulation," in 13th International IEEE Conference on Intelligent Transportation Systems, pp. 1468–1473, IEEE, 2010.
- [23] P. Liu, A. Kurt, and U. Ozguner, "Synthesis of a behavior-guided controller for lead vehicles in automated vehicle convoys," *Mechatronics*, vol. 50, pp. 366–376, 2018.
- [24] H. Zhang, L. Du, and J. Shen, "Hybrid MPC system for platoon based cooperative lane change control using machine learning aided distributed optimization," *Transportation Research Part B: Methodological*, 2021.
- [25] S. Mosharafian, M. Razzaghpour, Y. P. Fallah, and J. M. Velni, "Gaussian process based stochastic model predictive control for cooperative adaptive cruise control," in 2021 IEEE Vehicular Networking Conference (VNC), pp. 17–23, IEEE, 2021.
- [26] G. J. Naus, R. P. Vugts, J. Ploeg, M. J. van De Molengraft, and M. Steinbuch, "String-stable cace design and experimental validation: A frequency-domain approach," *IEEE Transactions on vehicular technology*, vol. 59, no. 9, pp. 4268–4279, 2010.
- [27] A. Bemporad and S. Di Cairano, "Model-predictive control of discrete hybrid stochastic automata," *IEEE Transactions on Automatic Control*, vol. 56, no. 6, pp. 1307–1321, 2010.
- [28] A. Bemporad and M. Morari, "Control of systems integrating logic, dynamics, and constraints," *Automatica*, vol. 35, no. 3, pp. 407–427, 1999
- [29] S. Diamond and S. Boyd, "CVXPY: A Python-embedded modeling language for convex optimization," *Journal of Machine Learning Research*, vol. 17, no. 83, pp. 1–5, 2016.
- [30] A. Agrawal, R. Verschueren, S. Diamond, and S. Boyd, "A rewriting system for convex optimization problems," *Journal of Control and Decision*, vol. 5, no. 1, pp. 42–60, 2018.
- [31] L. Gurobi Optimization, "Gurobi optimizer reference manual." http:// www.gurobi.com, 2021.



Sahand Mosharafian received his B.S and M.S in electrical engineering from K.N Toosi University of Technology, 2016, and University of Tehran, 2019, respectively. He has been a PhD student in electrical and computer engineering at the University of Georgia since August 2019. Currently, his research interests include connected and automated vehicles, optimization and control theory, and reinforcement learning.



Javad Mohammadpour Velni (Senior Member, IEEE) joined the University of Georgia, Athens, GA in 2012, where he served as an Associate Professor of Electrical Engineering until 2022. He was a Research Assistant Professor of mechanical engineering at University of Houston from 2008 to 2011 and a Research Investigator at the University of Michigan from 2011 to 2012. He has published over 200 articles in international journals and conference proceedings, served on the editorial boards of ASME and IEEE conferences on control systems

and edited two books on Control of Large-Scale Systems (2010) and LPV Systems Modeling, Control and Applications (published in 2012). His current research interests are in secure control of cyber-physical systems (and, in particular, transportation systems), coverage control of heterogeneous multiagent systems, and learning-based control of complex distributed systems. At the time of publication of this paper, he is a Professor of Mechanical Engineering at Clemson University, where he moved in August 2022.